Available online at www.sciencedirect.com
SCIENCE DIRECT®
International Journal of Heat and Mass Transfer 47 (2004) 1711–1718
International Journal of HEAT and MASS TRANSFER
www.elsevier.com/locate/ijhmt

Enhancement and reversal heat transfer by competing modes in jet impingement

F. Sarghini [a], G. Ruocco [b,*]

[a] DETEC, Università degli studi di Napoli Federico II, Italy
[b] DITEC, Università degli studi della Basilicata, Campus Macchia Romana, 85100 Potenza, Italy

Received 2 January 2003; received in revised form 20 October 2003

Abstract

A transient numerical analysis for fluid flow and heat transfer from a planar jet impingement on a finite thickness substrate is performed. A discrete heating boundary condition is applied to the substrate's under side; by including the effect of buoyancy, some assisting or opposing mixed convection configuration can be modelled and regions of momentum dominated, buoyancy dominated and unstable flows can be monitored. For low volumetric flows and small temperature differences, different competitive heat transfer modes can be detected, as conduction may affect heat transfer away from the impact site in the initial times, and flow pattern is driven by the ruling convective mechanism, whether forced or natural. The related flow field and local heat transfer rate are investigated as a function of a variety of geometry configurations, material coupling and thermal-fluid driving factors, for the unitary value of the mixed convection parameter *Ri* (transitional mixed convection).

Normalized heat transfer coefficients along the impinged substrate are reported by a parametric evaluation and may be employed to control the distribution of heat transfer at the given configuration. The inclusion of the conduction mechanism in the analysis confirms that the conjugate effect (heat transfer reversal) cannot be neglected during the initial exposition when an opposing cooling jet configuration is realized, for the largest investigated *Re*.

Keywords: Jet impingement; Conjugate heat transfer; Mixed convection; Local heat transfer

1. Introduction

Jet impingement (JI) is claimed to yield favorable heat transfer characteristics even for low volumetric flows. With ease of implementation, enhanced heat transfer rates are attained when a jet flow is directed from a nozzle of a give configuration to a target surface. JI flow structure can be summarized into three characteristic regions, shown in Fig. 1: the free jet region formed as jet exits with a velocity distribution $v(x)$, the impingement (stagnation) flow region formed upon jet impact and deflection, and the wall jet region formed upon re-acceleration of the flow along the confining surface. The wall jet may significantly contribute to the heat exchange in a conjugate configuration (simultaneous conduction in the target and convection by the jet flow), depending on target thickness and extent of heat transfer boundary. Either circular or planar nozzle geometry are usually employed, the choice being dictated by the fact that the slot jet provides a larger impingement zone, while the circular nozzle insures a more localized high transfer rate.

A reference to the most recent reviews by Jambunathan et al. [1] and Viskanta [2] for gaseous jets, or by Webb and Ma [3] for liquid jets, among others, can be made for a survey of configurations and comparison of theoretical and experimental JI works. JI studies are sustained by a considerable interest due to its potential

* Corresponding author. Tel.: +39-0971-205454; fax: +39-0971-205429.
E-mail address: ruocco@unibas.it (G. Ruocco).

0017-9310/$ - see front matter © 2003 Elsevier Ltd. All rights reserved.
doi:10.1016/j.ijheatmasstransfer.2003.10.015

Nomenclature

c_p	specific heat at constant pressure, kJ kg^{-1} K^{-1}
g	gravitational acceleration constant, m s^{-2}
Gr	Grashof number, dimensionless
k	thermal conductivity, W m^{-2} K^{-1}
K	thermal conductivity ratio, dimensionless
l	domain length, m
L	dimensionless domain length
p	pressure, Pa
P	dimensionless pressure
Nu	Nusselt number, dimensionless
Pr	Prandtl number, dimensionless
Re	Reynolds number, based on nozzle width, dimensionless
Ri	Richardson number, dimensionless
t	temperature, K
T	dimensionless temperature
u	x-component velocity, m s^{-1}
U	dimensionless x-component velocity
v	y-component velocity, m s^{-1}
V	dimensionless y-component velocity
x	coordinate, m
X	dimensionless coordinate
y	coordinate, m
Y	dimensionless coordinate
w	jet width, m

Greek symbols

γ	coefficient in Eq. (3)
μ	dynamic viscosity, Pa s
ρ	density, kg m^{-3}
θ	time, s
Θ	dimensionless time

Subscripts

c	heating component
f	fluid sub-domain
j	jet
s	solid sub-domain
∞x	undisturbed, along x
∞y	undisturbed, along y

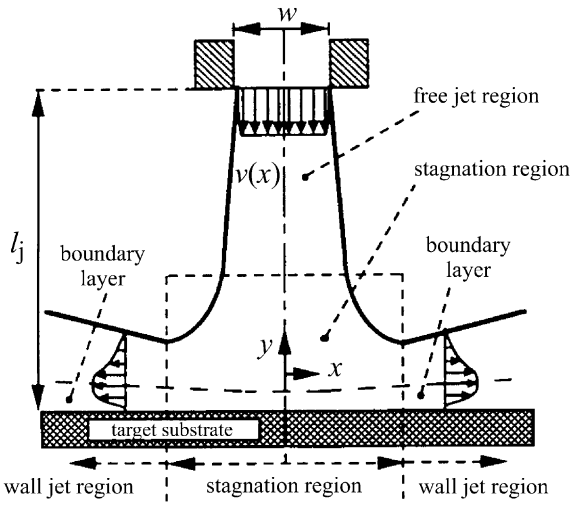

Fig. 1. Jet impingement flow regions.

application in industrial thermal control and material processing and conditioning. JI offers these favorable characteristics even for low volumetric flows, as in chemical vapor deposition (CVD). In a recent experimental report by Mathews and Peterson [4], a carrier gas is used in semiconductor manufacturing to deliver silicon to the surface of a substrate wafer. Higher quality, uniformity and growth rate of deposited film are ensured by the knowledge of the heat transfer local rate and carrier gas stability conditions, in turn dictated by secondary flow patterns favored by the inherent buoyancy. The control of a heat or mass flux distribution rate along the impinged surface is an additional favorable JI feature, yet the occurrence of competition between transfer of heat by conduction in the substrate and by convection in the fluid can alter this distribution, indicating the need of a more realistic modelling approach.

Despite the large body of literature on JI, as most work has been limited to the fluid region, there is a lack of knowledge of the conjugated mechanisms that drive the enhancement of heat transfer, when an aiding/opposing jet-surface orientation is adopted, or its reversal, when concurrent substrate conduction is present. The transitional convective regime, i.e. the pure natural and the pure forced convection mechanisms are of the same order of magnitude [5], is a specially interesting case.

Starting with the pioneer works by Wang et al. [6–9], these and two other research groups [10–12] have carried out studies on the conjugate effect for laminar, non-buoyant JI under the assumption of uniform heating of the solid region, but in more realistic configurations the influence of discrete boundary conditions on JI heat transfer are certainly relevant. Under the discrete b.c. assumption, Schafer et al. [13] first provided measurements for the heat transfer relative to a laminar slot jet to cool an array of discrete, flush-mounted heat sources in a channel, then performed a numerical simulation relative to the same arrangement under a laminar JI [14],

although the generality of the study of the conjugate effect was limited, due to the absence of competing conduction. Their findings confirmed the relative merit of dimensionless geometry and solid–fluid coupling parameters, such as Prandtl number and conductivity ratio. Manca et al. [15] noticed the occurrence of the reversal effect, found by a numerical simulation. For a laminar confined JI, the effect of the solid thickness and the extent of a heating source is such that the substrate helps diffuse heat away from the stagnation region, but starting from a certain distance downstream, the heat is transferred back to the solid. For a similar configuration and using the same approach, Ruocco [16] investigated the conjugate heat transfer mechanism and fluid flow patterns in detail, by reporting their 3-D representations relative to air or water confined JI coupling with an alumina plate. Then again, Ruocco [17] inferred the relationship between total generated entropy and average heat transfer rate, for a still similar configuration, based on solid–fluid coupling characteristics. Finally, Bula et al. [18] analyzed by a finite element technique the conjugate heat transfer to an heated disk impinged by a laminar liquid jet, finding that the disk thickness and heating sectors locations strongly influence the local heat transfer rate.

When the inlet flow velocity is relatively low and the temperature difference between the target surface and the flowing fluid is large enough, the velocity and temperature fields are strongly influenced by buoyancy. This is particularly important to the alteration of the recirculation pattern that is formed by the jet flow upon interaction with the substrate surface. A variety of assisting or opposing flows may be therefore conceived, depending on jet-surface temperature difference and surface orientation, and heat and mass transfer enhancement is likely to occur under these assumptions. A first study on buoyancy effect to pure fluid JI has been presented by Yuan et al. [19], who primarily found a substantial heat transfer enhancement for high Richardson number conditions, and jet offset peaks in the Nusselt number distribution. Later, Wang et al. [20] studied numerically a non-confined circular JI on a heated surface. They found that the Nusselt number is considerably influenced by natural convection only in the case of large difference between the initial gas temperature and the substrate temperature and at low Reynolds number, with detrimental effects on the heat transfer at the stagnation point. Finally, Potthast et al. [21] also performed mixed convection simulations relative to confined axial or radial JI. They found that free convection may influence the JI on a horizontal plate by increasing the heat transfer, and obtained periodic solution for the smallest Grashof number and chaotic flow for the largest Grashof number.

As mentioned in the above, the alteration of JI flow structure due to buoyancy, and its impact on competing conduction is still largely unexplored. Altieri et al. [22] assessed, for few noteworthy configurations, the local Nusselt number distributions due to assisted and opposed impinging jets along the impinged substrate. The present numerical work is intended to extend such analysis to describe the enhancement and reversal of heat transfer in a discretely heated, finite thickness substrate, placed into an unconfined space, impinged by a flow in transitional mixed convection ($Ri = Gr/Re^2 = 1$). To this end, the thermal and flow fields are determined by resolving the impact boundary layer in such peculiar mixed convection configuration, while special care is used to ensure convergence for assisting or opposing flows.

2. Analysis

In this work a cooling impinging jet discharges vertically from an adiabatic feed tube into an unconfined space, limited by a heated solid substrate (included in the domain), with a fully developed profile. The examined arrangement is drawn in Fig. 2, where only half section of the domain is considered due to the geometry and thermal symmetries. The following assumptions are adopted: (1) The flow is laminar, due to the choice made on the dimensionless mixed convection parameter, which will be discussed in the next section. (2) The flow is two-dimensional and incompressible with constant properties, while the variation of density with temperature is only allowed to account for the Boussinesq approximation. (3) The viscous heat dissipation is neglected. (4) A constant temperature condition is applied to a sector of impinging plate's under side, and no-slip is considered to its upper side. (5) The outer boundaries of

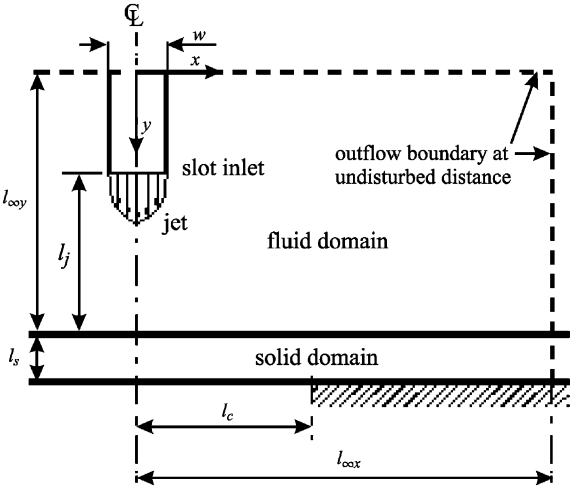

Fig. 2. Study domains and nomenclature (not to scale).

the system are considered adiabatic, and relative momentum conservation equations are rendered locally parabolic, as the corresponding normal-wise diffusion is assumed to be zero. (6) The thermal-fluid boundary conditions imposed at the feed tube inlet are such that the contingent effect of buoyancy on jet discharge (flow reversal in the tube) is not considered.

With reference to the previous statements the governing dimensionless equations of conservation, in Cartesian coordinates, are:

Continuity:

$$\frac{\partial U}{\partial X}+\frac{\partial V}{\partial Y}=0 \tag{1}$$

Momentum in the x-direction:

$$\frac{\partial U}{\partial \Theta}+U\frac{\partial U}{\partial X}+V\frac{\partial U}{\partial Y}=\frac{1}{Re}\left(\frac{\partial^2 U}{\partial X^2}+\frac{\partial^2 U}{\partial Y^2}\right)-\frac{\partial P}{\partial X} \tag{2}$$

Momentum in the y-direction:

$$\frac{\partial V}{\partial \Theta}+U\frac{\partial V}{\partial X}+V\frac{\partial V}{\partial Y}=\frac{1}{Re}\left(\frac{\partial^2 V}{\partial X^2}+\frac{\partial^2 V}{\partial Y^2}\right)-\frac{\partial P}{\partial Y}+\gamma Ri\,T \tag{3}$$

with $\gamma=+1$ or -1, for the upward facing jet (aiding convection) or the downward facing jet (opposing convection).

Energy in fluid sub-domain:

$$\frac{\partial T}{\partial \Theta}+U\frac{\partial T}{\partial X}+V\frac{\partial T}{\partial Y}=\frac{1}{RePr}\left(\frac{\partial^2 T}{\partial X^2}+\frac{\partial^2 T}{\partial Y^2}\right) \tag{4}$$

Energy in solid sub-domain:

$$\frac{\partial T}{\partial \Theta}=\frac{\partial^2 T}{\partial X^2}+\frac{\partial^2 T}{\partial Y^2} \tag{5}$$

The following dimensionless quantities and coefficients are defined:

$$\begin{aligned}
&\Theta=\frac{\theta v_j}{w};\quad X=\frac{x}{w};\quad Y=\frac{y}{w};\quad L=\frac{l}{w};\\
&U=\frac{u}{v_j};\quad V=\frac{v}{v_j};\quad P=\frac{p-p_{\infty x,y}}{\rho v_j^2};\quad T=\frac{t-t_j}{t_c-t_j};\\
&Gr=\frac{\rho_j^2 g(t_c-t_j)w^3}{t_j\mu_j^2};\quad K=\frac{k_s}{k_f};\quad Re=\frac{\rho_j v_j w}{\mu_j};\\
&Pr=\frac{c_{pj}\mu_j}{k_j};\quad Ri=\frac{Gr}{Re^2}
\end{aligned} \tag{6}$$

2.1. Boundary conditions

The initial condition, in both solid and fluid domains, is the following:

$$\begin{aligned}
&U=0,\quad V=0 \quad \text{in the fluid domain}\\
&T=0 \quad \text{in both domains}
\end{aligned} \tag{7}$$

The boundary conditions are defined as follows:

Jet inlet ($0\leqslant X\leqslant 0.5$, $Y=L_{\infty y}-L_j$):

$$U=0,\quad V=1.5(1-4X^2),\quad T=0 \tag{8}$$

Fluid symmetry plane ($X=0$, $L_{\infty y}-L_j<Y<L_{\infty y}$):

$$U=0,\quad \frac{\partial V}{\partial X}=0,\quad \frac{\partial V}{\partial X}=0 \tag{9}$$

Substrate symmetry plane ($X=0$, $L_{\infty y}\leqslant Y<L_{\infty y}+L_s$):

$$\frac{\partial T}{\partial X}=0 \tag{10}$$

Feed tube wall ($X=0.5$, $0\leqslant Y<L_{\infty y}-L_j$):

$$U=0,\quad V=0,\quad \frac{\partial T}{\partial X}=0 \tag{11}$$

Substrate–fluid interface ($0<X\leqslant L_{\infty x}$, $Y=L_{\infty y}$):

$$U=0,\quad V=0,\quad T_f=T_s,\quad \frac{\partial T_f}{\partial Y}=K\frac{\partial T_s}{\partial Y} \tag{12}$$

Fluid, at undisturbed distance along X ($X=L_{\infty x}$, $0<Y<L_{\infty y}$):

$$V=0,\quad \frac{\partial U}{\partial X}=0,\quad \frac{\partial T}{\partial X}=0 \tag{13}$$

Fluid, at undisturbed distance along Y ($0<X\leqslant L_{\infty x}$, $Y=0$):

$$U=0,\quad \frac{\partial V}{\partial Y}=0,\quad \frac{\partial T}{\partial Y}=0 \tag{14}$$

Substrate, at undisturbed distance ($X=L_{\infty x}$, $L_{\infty y}\leqslant Y<L_{\infty y}+L_s$):

$$\frac{\partial T}{\partial X}=0 \tag{15}$$

Substrate back side, constant temperature sector ($0<X\leqslant L_c$, $Y=L_{\infty y}+L_s$):

$$T=1 \tag{16}$$

Substrate back side, adiabatic sector ($L_c<X<L_{\infty x}$, $Y=L_{\infty y}+L_s$):

$$\frac{\partial T}{\partial X}=0 \tag{17}$$

2.2. Numerical method and additional considerations

A SIMPLEC procedure is employed to integrate the governing equations with related boundary conditions, whose details are reported in [22] including the algebraic solver, except for the time dependance which is enforced

in this study. The effect of the different values of solid domain lengths $L_{\infty x}$ and $L_{\infty y}$ has first been monitored, to enforce boundary conditions (13) and (14), and the optimal values of 20 and 16 was respectively selected. Once the flow field is obtained by solving Eqs. (1)–(3) in the fluid domain, the thermal field can be calculated by solving Eqs. (4) and (5) in both domains; a harmonic mean is used at the domain interface to deal with the discontinuity in the thermal conductivity.

The final solution for each time step is then iteratively sought updating the driving parameters Gr and Re, which form the mixed convection parameter Ri, and the thermodynamic property parameter Pr. In fact, according to the scale analysis reported in the textbook by Bejan [5], the dimensionless groups that serve as criterion for transition from natural to forced convection are

$$Ri^{0.25}\begin{cases} > 1, & \text{natural convection} \\ < 1, & \text{forced convection} \end{cases} \quad \text{for fluids with } Pr < 1 \tag{18}$$

and

$$\frac{Ri^{0.25}}{Pr^{0.083}}\begin{cases} > 1, & \text{natural convection} \\ < 1, & \text{forced convection} \end{cases} \quad \text{for fluids with } Pr > 1. \tag{19}$$

A stretched grid of 100×90 has been employed, in all computations, to resolve the velocity and pressure gradients in the boundary layer, induced by the impingement and redirection of flow. A grid-independence positive check has also been performed on a 180×140 grid. The time step has been kept consistently small to ensure stability. Convergence of the numerical results, for each time step, is assumed when the maximum absolute difference between two consecutively iterated solution sets is within 10^{-4} for U, V and P, and 10^{-6} for T.

Once the thermal field is obtained, the local Nusselt number can be evaluated at the solid–fluid interface, by using a 4-point Lagrangian interpolation of dimensionless temperature derivative calculated at domain interface:

$$Nu_x = -\left(\frac{\partial T}{\partial Y}\right)_{Y=L_{\infty y}} \tag{20}$$

Then a normalized heat exchange coefficient can be formed as $Nu_x/(Re^{1/2}Pr^{1/3})$. Except when transient solutions are sought, a steady state is reached as Nu is kept within 10^{-3} between two consecutive time steps. The validation of the model has been reported in [22] through comparison of Nu distributions, against the pure fluid calculations at steady state of Yuan et al. [19] for a heated air jet. Only qualitative agreement has been found, as the flow domain adopted by [19] was critically limited and presumably could not account for specific topologies such as wall or plume flows.

For the present calculations a mixed convection condition has been enforced as described by (18) or (19), and a geometry and fluid dynamic base-case has been set: $L_c = 0.5$, $L_s = 0.25$, $L_j = 2.0$, $Re = 10$. Various material coupling has been explored by setting K for the following combinations: epoxy fiberglass–water: 4.44×10^{-1}, alumina–water: 2.83×10^{2}, alumina–air: 6.29×10^{3}. As usual, Pr was set as 0.71 or 6.5 for air or water, respectively.

3. Results and discussion

A number of parameters have been monitored that affect local heat transfer in the jet vicinity, by keeping the nozzle height L_j and the component width L_c as constants. In Figs. 3 and 4 two typical combinations of flow and temperature fields at steady state are presented,

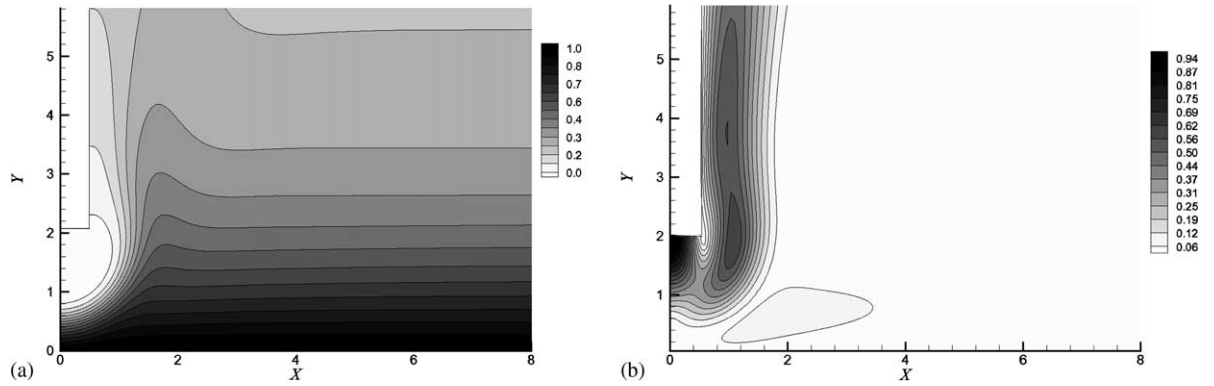

Fig. 3. Base case, with $Re = 50$ for air impinging on alumina in opposing mixed convection: temperature distribution (a) and velocity field (b).

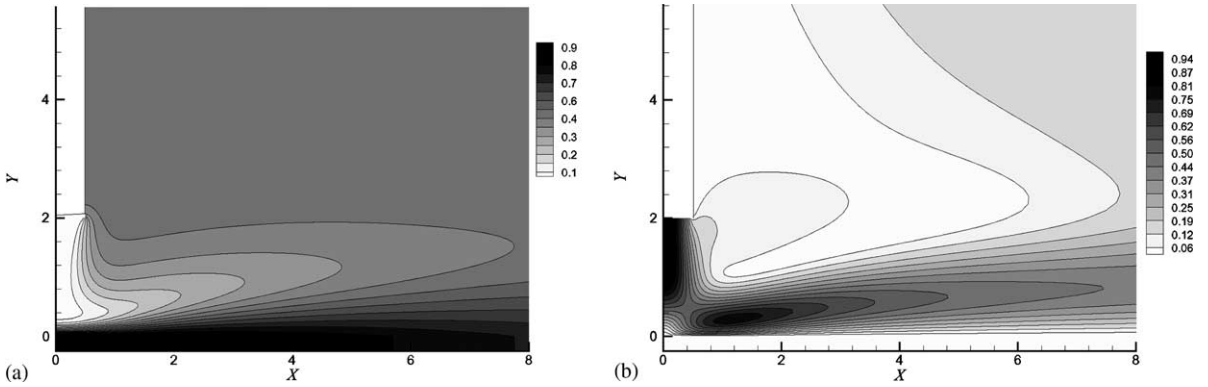

Fig. 4. Base case, with $Re = 50$ for air impinging on alumina in aiding mixed convection: temperature distribution (a) and velocity field (b).

to illustrate their variation to jet orientation. In particular, it is seen in Figs. 3a and 4a that the solutions for T include the distribution in the substrate; in Fig. 3b is then seen how the plume develops along the nozzle wall side, when a downward jet is configured, while for the upward configuration Fig. 4b evidences the usual wall jet, accelerating upon impingement (forming the stagnation region) and redirection.

The local heat transfer rate is examined first by studying the jet orientation, for two different Re numbers. In Fig. 5a such effect is displayed: it is evident, as expected, that the upward facing jet ($\gamma = +1$) offers inherently higher heat transfer rates but the normalized heat transfer gets worse for increasing Re. This is due to the fact that, in order to keep $Ri = 1$, the temperature boundary condition value had to conform, but much less than the increase in Re, and consequently is the heat transfer rate. Moreover, starting at approximately $X = 2.9$ the downward jet (aiding convection) performs better that the upward one for $Re = 10$, as the effect of the wall jet is found on the substrate, while for $Re = 50$ this happens much later along the substrate (about $X = 4.2$, not shown) as the jet interacts more effectively with the surface before being redirected upward as a plume (as in Fig. 3).

The analysis of the effect of jet orientation is completed by Fig. 5b, in which the effect of two different choices of substrate thickness is monitored on local heat transfer. Here the effect of halving the thickness produces a decrease of the heat transfer rate, along the entire impinged surface, as a result of the added resistance to conduction. A conjugate effect (competition of conduction and convection) is seen for both substrate thickness in aiding convection, as secondary maxima are found for $X = 4.3$ and 6.0 when L_s are 0.125 and 0.25, respectively: the additional conduction resistance at the smaller thickness induces an earlier occurrence of this phenomenon. Finally, conjugate effect is not present for the downward jet, at any thickness, and the heat transfer is independent on L_s for $X > 6$.

The effect of material conductivity coupling is monitored instead in Fig. 6a for the upward facing jet. As

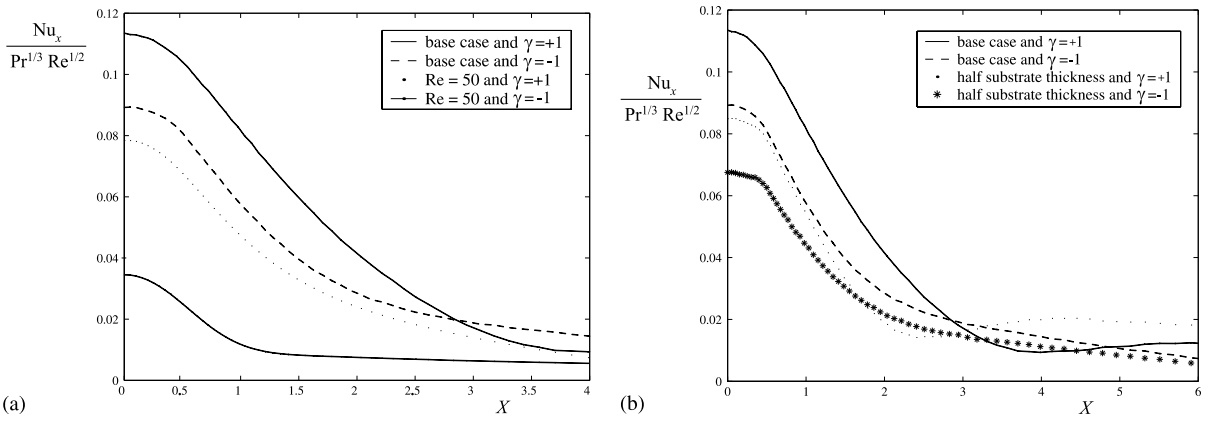

Fig. 5. Effect of jet orientation in mixed convection: varying Re (a), or the substrate thickness (b).

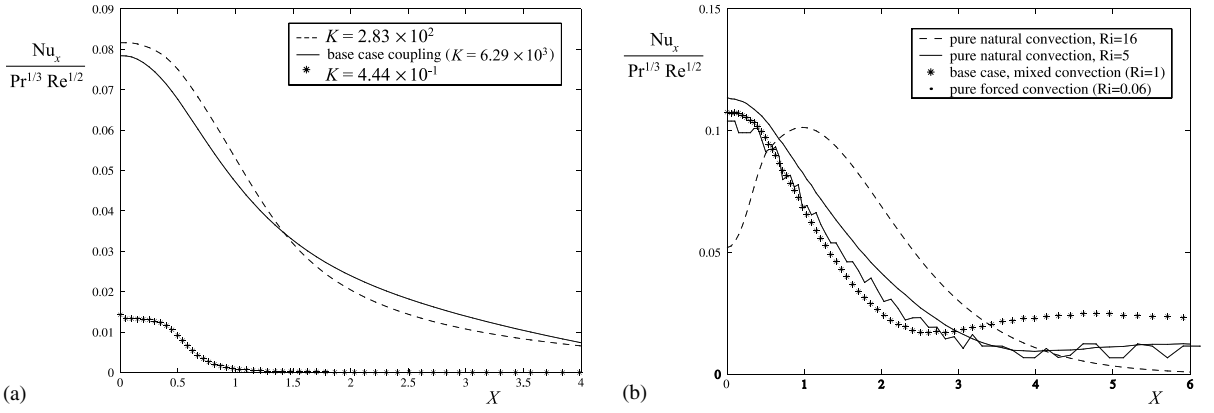

Fig. 6. Effect of conductivity coupling K (a), and convective mechanisms competition Ri (b) in aiding convection (upward facing jet, $\gamma = +1$).

the heat transfer increase is not exactly monotone with the dimensionless conductivity parameter K, one can infer that this parameter is not an adequate descriptor for the problem at hand, that is, the local heat transfer is mostly dependent on transport rather than diffusion. Even so, the effect of a scarcely conductive substrate (epoxy fiberglass, $K = 4.44 \times 10^{-1}$) to a water jet is largely felt as the heat transfer is several times smaller than the case when alumina is employed instead ($K = 2.83 \times 10^2$).

The competition of different convective mechanisms is presented in Fig. 6b, again for the upward facing jet. A large plume forms an off-set maximum when strong natural convection only is configured ($Ri = 16$). The figure evidences that the progress is barely monotone with Ri, and steady-state solutions were hardly found for large values of this parameter, confirming the findings of Potthast et al. [21]. The intermittent progress in pure forced convection ($Ri = 0.06$) is an artifact due to the Nu approximation for a very small temperature difference between jet and heated plate.

The transient behavior of the configuration at hand is reported in the last set of figures. It is instructive to note that for many configurations the conjugate effect, that is the competitive effect of conduction over convection, is found starting from the stagnation for various lengths in the very first moments of substrate exposition. The heat transfer reversal (the heat flux is directed from the flow to the plate) vary with time very similarly depending on different solid thickness, as is monitored in Fig. 7. the effect of different solid thickness is first monitored. When the effect of reverse orientation is examined instead, as in Fig. 8, the progresses differ greatly but it is more effective for a downward facing jet.

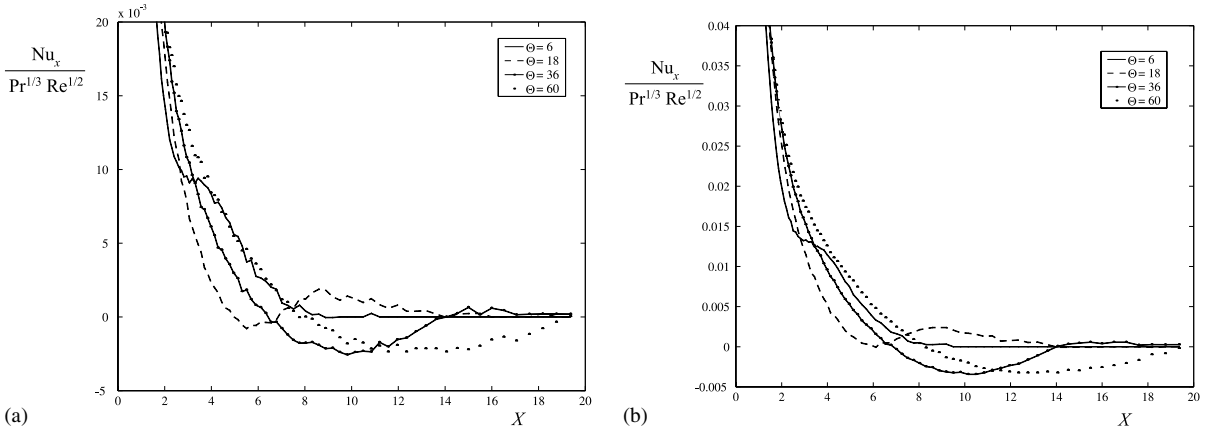

Fig. 7. Transient local normalized heat transfer distribution $L_s = 0.125$ (a), and $L_s = 0.25$ (b) in aiding convection (upward facing jet, $\gamma = +1$).

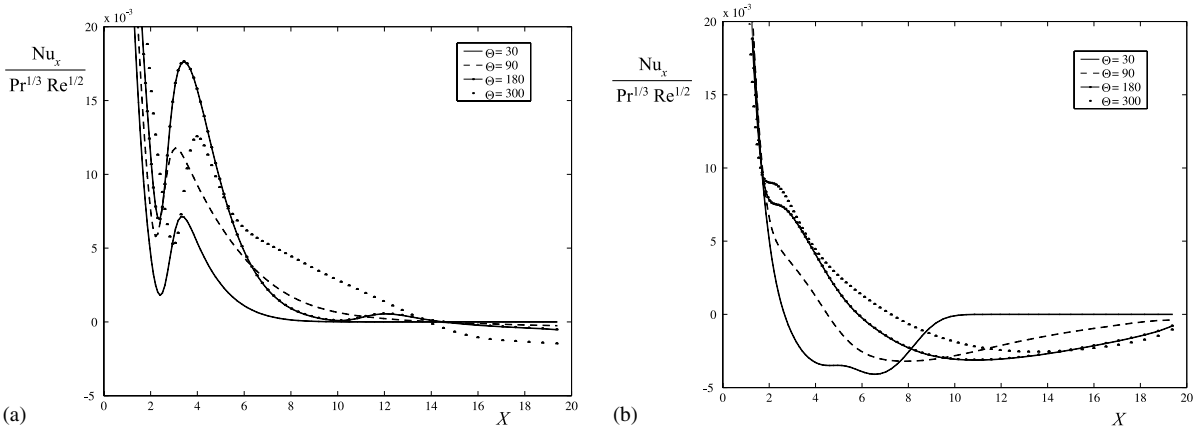

Fig. 8. Transient local normalized heat transfer distribution for $Re = 50$ in aiding convection (upward facing jet, $\gamma = +1$) (a), and in opposing convection (downward facing jet, $\gamma = -1$) (b).

4. Conclusions

A parametric numerical analysis has been conducted to infer on the competition between different heat transfer modes in laminar JI on a finite thickness, discretely heated substrate. Several effects have been monitored such as jet orientation, *Re*, substrate thickness, material coupling in mixed, pure forced or pure natural convection. Heat transfer is locally evaluated depending on such effects, whose inclusion must be made in any analysis in order to yield correct predictions on the studied configuration. Transient heat transfer distribution show the presence of heat transfer reversal which has to be considered in those processes, as in CVD, where is certainly appreciable and product-sensitive.

Acknowledgements

This work was funded by MIUR Italian Ministry of Scientific Research, grant no. 2002093829 entitled "Aspetti fondamentali ed applicativi dei getti sommersi nelle tecniche innovative di scambio termico—Visualizzazione e simulazione integrate per la valutazione dello scambio termico da getti impingenti su piastre in configurazioni innovative".

References

[1] K. Jambunathan, E. Lai, M.A. Moss, B.L. Button, Int. J. Heat Fluid Flow 13 (1992) 106.
[2] R. Viskanta, Exp. Thermal Fluid Sci. 6 (1993) 111.
[3] B.W. Webb, C.F. Ma, in: Advances in Heat Transfer, 26, Academic Press, New York, 1995, p. 105.
[4] A.G. Mathews, J.E. Peterson, ASME J. Heat Transfer 124 (2002) 564.
[5] A. Bejan, Convection Heat Transfer, John Wiley & Sons, 1995.
[6] X.S. Wang, Z. Dagan, L.M. Jiji, Int. J. Heat Mass Transfer 32 (7) (1989) 1351.
[7] X.S. Wang, Z. Dagan, L.M. Jiji, Int. J. Heat Mass Transfer 32 (7) (1989) 1361.
[8] X.S. Wang, Z. Dagan, L.M. Jiji, Int. J. Heat Mass Transfer 32 (11) (1989) 2189.
[9] X.S. Wang, Z. Dagan, L.M. Jiji, ASME J. Electr. Packgng. 112 (1990) 57.
[10] A. Faghri, S. Thomas, M.M. Rahman, ASME J. Heat Transfer 115 (1993) 116.
[11] M.K. Alkam, P.B. Butler, J. Thermophys. Heat Transfer 8 (4) (1994) 664.
[12] M.M. Rahman, A.J. Bula, J.E. Leland, J. Thermophys. Heat Transfer 14 (3) (2000) 330.
[13] D.M. Schafer, F.P. Incropera, S. Ramadhyani, ASME J. Electr. Packgng. 113 (1991) 359.
[14] D.M. Schafer, S. Ramadhyani, F.P. Incropera, Numer. Heat Transfer Part A 22 (1992) 121.
[15] O. Manca, V. Naso, G. Ruocco, Conjugate heat transfer to a laminar confined impinging planar jet, in: L.C. Wrobel et al. (Eds.), Advanced Computational Methods in Heat Transfer IV, Computational Mechanics Publications, Ashurst Lodge, UK, 1996, pp. 149–158.
[16] G. Ruocco, Int. J. Heat Technol. 15 (2) (1997) 41.
[17] G. Ruocco, Int. Commun. Heat Mass Transfer 24 (2) (1997) 201.
[18] A.J. Bula, M.M. Rahman, J.E. Leland, Int. J. Heat Fluid Flow 21 (1997) 11.
[19] T.D. Yuan, J.A. Liburdy, T. Wang, ASME J. Heat Transfer 31 (10) (1988) 2137.
[20] Y.B. Wang, C. Chaussavoine, F. Teyssandier, Int. J. Heat Mass Transfer 36 (1993) 857.
[21] F. Potthast, H. Laschefski, N.K. Mitra, Numer. Heat Transfer Part A 26 (1994) 123.
[22] G. Altieri, V. De Luca, G. Ruocco, Buoyancy effects on conjugate heat transfer due to a laminar impinging jet: Preliminary results, in: Proceedings, 5th ASME/JSME Joint Thermal Engineering Conference, San Diego, USA, March 1999, pp. 15–19.